Crystal structure of the PSPTO-PSP protein from *Pseudomonas syringae pv. tomato str. DC3000* in complex with D-glucose

Hong-mei Zhang, Yu Gao, Mei Li, Wen-rui Chang *

National Laboratory of Biomacromolecules, Institute of Biophysics, Chinese Academy of Sciences, 15 Datun Road, Chaoyang District, Beijing 100101, PR China

ARTICLE INFO

ABSTRACT

The perchloric acid-soluble protein (PSP) is an endoribonuclease and on the basis of sequence similarity has been assigned to the YjgF/YER057c/UK114 family. These family members are ubiquitous and highly conserved in evolution, and participate in regulating basic cellular metabolism. Here we present the 2.1 Å crystal structure of the PSP protein from *Pseudomonas syringae pv. tomato str. DC3000* (PSPTO-PSP), in complex with D-glucose. The quaternary structure of PSPTO-PSP is a homologous trimer. Glucose is located in the cavity between each two monomers. Comparison of the hydrogen bonds between ligands and YjgF/YER057c/UK114 family homologues confirms that the conserved Arg[103] of PSPTO-PSP is a key amino acid in this cavity for ligand binding. It indicated that the involvement of PSPTO-PSP in essential cellular mechanism was regulated by glucose occupying this active site.

© 2010 Elsevier Inc. All rights reserved.

1. Introduction

The perchloric acid-soluble protein from *Pseudomonas syringae pv. tomato str. DC3000* (PSPTO-PSP) contains 126 amino acids and has been assigned to the YjgF/YER057c/UK114 family based on sequence similarity. A high level of sequence identity between members of this family, which includes different species from single-celled to multicellular organisms, implies that this family of proteins is ubiquitous and highly conserved in evolution. The functions of family members are broad, including isoleucine and purine biosynthesis, L-threonine deamination, mitochondrial maintenance, and protein synthesis inhibition [1–4].

Some members, such as the UK114 protein from goat liver, hp14.5 protein from human monocytes and perchloric acid-soluble protein (L-PSP) from rat liver, have been characterized as translational inhibitors [5,6]. The L-PSP of mouse has shown an inhibitory activity on cell proliferation [7]. The expression of PSP in rat hepatoma was down regulated as comparing with intact tissue, but was up regulated in the central of region of tumor tissue [8]. A human homologue named hp14.5 isolated from monocytes was described as a translational inhibitor which undergoes up-regulation during cellular differentiation [6]. All these results from different laboratories show a fact that PSP expression has an opposite relationship with the cellular protein synthesis, and that PSP is involved in cellular growth and differentiation.

This inhibitory activity of PSP on protein synthesis results from its ribonuclease activity which inhibits the initial steps of transla-

tion. It has been reported that rat L-PSP has endoribonuclease activity and its specific substrate is mRNA, rather than rRNA or tRNA. This activity is not inhibited by cycloheximide, suggesting that L-PSP protein is unique among liver RNAase's [9].

Rat P23, a homologue of PSP, which belongs to the YjgF family, has 100% identity with rat L-PSP from amino acids 38–136. P23 mRNA expression in the liver of starved animals was enhanced, but decreased when glucose was added to the diet for 1 day before sacrifice [10]. In addition, L-PSP is a fatty acid-induced protein. Intestinal L-PSP expression increases approximately 3-fold by oral administration of dietary fat [11]. L-PSP protein extracted from rat liver contains six major fatty acid components identified by GC-MS lipid analysis [12]. These various results show that the expression of L-PSP is regulated by nutrients and that L-PSP is related to glucose and lipid metabolism.

Even though it has been reported that some nutrients affect PSP mRNA expression, there are still no structures or other biochemical proofs available to help elucidate how glucose, fatty acids or other nutrients regulate PSPs. Here, the 2.1 Å crystal structure of PSPTO-PSP in complex with glucose showed that the inhibition of PSP on protein synthesis might be regulated by glucose directly occupying PSPs' active site. This complex structure supported the Levy–Favatier's proposal [10].

2. Materials and methods

2.1. Protein expression, purification, crystallization and data collection

Recombinant PSPTO-PSP was expressed with an N-His-tag using the Phat2 plasmid in *Escherichia coli* BL21 cells. Expressed

---

proteins were bound to Ni–NTA beads, eluted with 250 mm imid-azole, and further purified by anion exchange (R-source Q™) and size exclusion (Superdex™ 75) chromatography. The purity of PSPTO-PSP was over 95%.

Crystals were obtained using the hanging drop vapor diffusion method with a 1:1 mixture of protein (10 mg/ml protein in 5 mM Tris–HCl, 50 mM NaCl, pH 8.0) and reservoir solution (PEG8000 20%, 0.05 M $NaKHPO_4$). Needle-like crystals appeared after 1 month. The optimized crystal was grown in a well solution of 26% PEG8000, 0.05 M $NaKHPO_4$, and 15% D-glucose, and matured after 1 month. The crystal was cryo-protected with a 7:3 mixture of paraffin oil and NVH oil prior to freezing in nitrogen vapor. The data were collected to 2.1 Å at 100 K on the Rigaku FR-E Vari-Max at the Institute of Biophysics, Chinese Academy of Sciences, Beijing. Data were processed by HKL2000 [13] and are shown in Table 1.

2.2. Solving the crystal structure

The structure of PSPTO-PSP was solved by the molecular replacement method using the program PHASER [14] and the coor-dinates of *Bacillus subtilis* YabJ (PDB code 1QD9, 49% sequence identity to PSPTO-PSP). PHASER was run with a resolution range of 20.0–2.1 Å in the space group $P2_12_12_1$. Five percent of the reflec-tions were excluded from the total for cross-validation with the Rfree value. A crude model was built using the ARP/wARP program [15]. The rigid-body model was initially refined with the program Refmac5, and several cycles of manual model rebuilding and model refinement were then performed using Coot and Refmac5 [16,17]. Water molecules were automatically detected by the ARP/wARP

Table 1
Summary of X-ray data and model parameters for PSPTO-PSP.

Dataset	Data
Wavelength	1.5418 Å
Cell parameters	$a = 66.89$ Å, $b = 75.71$ Å, $c = 79.30$ Å
Resolution	20–2.1 (2.1) Å
Unique reflections	23,719
Completeness	97.9% (96.2%)
Redundancy	13.1 (13.1)
R_{merge}[a,b]	0.08 (0.34)
$<I/\sigma(I)>$[a]	35.6 (8.0)
Refinement	
R_{work}[c] (based on 95% of data; %)	18.06
R_{free}[c] (based on 5% of data; %)	23.40
Ramachandran plots[d] (%)	99.2
R_{msd} bond distances (Å)	0.009
R_{msd} bond angles (°)	1.554
Contents of model	
Protein (residues)	370
Water (molecules)	248
Ligands	3
Ligand (identity[e]/sites occupied)	BLC/D–F
Average temperature factors ($Å^2$)	
Main-chain atoms	21.01
Side-chain atoms	23.8
Water molecules	29.9
Ligand molecules	29.6
Overall	22.48
PDB accession code	3K0T

[a] The figures in brackets indicate the values for the outer resolution shell.
[b] $R_{merge} = \Sigma h \Sigma l |Ihl - <Ih>|/\Sigma h \Sigma l < Ih>$, where Il is the lth observation of reflec-tion, and h and < Ih > is the weighted average intensity for all observations l of reflection h.
[c] R-factors and R_{free} were calculated as follows: $R = \Sigma (|F_{obs} - F_{calc}|)/\Sigma |F_{obs}| \times 100$, where F_{obs} and F_{calc} are the observed and calculated structure factor amplitudes, respectively.
[d] Residues with most favoured Φ/Ψ angles as calculated using PROCHECK.
[e] BGC = D-β-glucose.

program, and confirmed based on peak heights and distance crite-ria in the Fo-Fc and 2Fo-Fc maps. The quality of the model was evaluated with Procheck [18]. The coordinates have been depos-ited in the Protein Data Bank (Accession number (3K0T). Data col-lection and refinement data are summarized in Table 1.

3. Results and discussion

3.1. Overall structure of PSPTO-PSP

PSPTO-PSP is patterned as a trimer in an asymmetrical unit, each subunit of which shows an α + β fold with a β β βα β α β β arrangement. β4 and β5 are parallel, and all other strands in the sheet are anti-parallel. Two parallel α-helices are opposite to the β sheet (Fig. 1A). The center of the trimer is an empty triangular barrel-like conformation, the bottom of which is comprised of three long and meandering loops from three subunits while the top is open. Twelve longer β strands form the inner surface and the surrounding α-helices form the outer surface of the barrel (Fig. 1B). A deep cavity in the interface between each two subunits contains a D-glucose.

3.2. The triangular barrel-like cavity of the PSPTO-PSP trimer

Viewed from top to bottom, the barrel is comprised of four interacting layers (Fig. 2a). The body of the barrel consists of a hydrophobic layer, and a hydrophilic layer located between the cover and bottom hydrophobic layers. The barrel is covered by three Tyr[29] and three Ile[122] residues and one water molecule (Fig. 2b). Three hydrogen bonds are formed between the water molecule and the three Tyr[29]. The benzene rings of the three Tyr[29], and three Ile[122] (one from each subunit) have hydrophobic interaction (Fig. 2b). The hydrophilic layer includes three sets of Lys[74,] Asn[76], Asp[120] (one set from each subunit) arranged in a circle, with a hydrogen bond formed between each neighboring amino acid (Fig. 2c). The following hydrophobic layer is composed of three sets of Phe[78] and Ile[106] (Fig. 2d). The bottom of the barrel is sealed by three Ala[109] and three Val[108] (Fig. 2e). All these amino acids, highly conserved in evolution, maintain the stability of the trimer by strong hydrogen bonds and hydrophobic interactions.

In addition, hydrophobic interactions occur between the Ile[22] of one subunit and the Val[73] of the adjoining subunit. Hydrogen bonds between the oxygen of Ser[31] and the oxygen or nitrogen of Arg[103] from neighboring subunits locked adjoining subunits, sealed
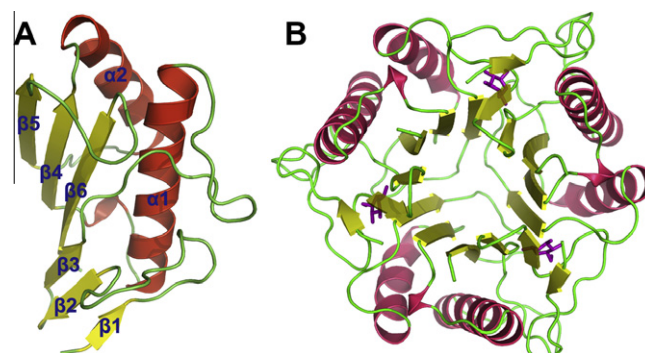

Fig. 1. Cartoon diagram of the PSPTO-PSP. Panel A is the monomer; panel B is the trimer in complex with glucose. The inner surface of the barrel-like cavity of the trimer consists of 12 β-strands (yellow), and the outer surface consists of two α-helices (red).Glucose is bound as a ligand (purple). The loop is shown as green. (For interpretation of the references to color in this figure legend, the reader is referred to the web version of this article.)
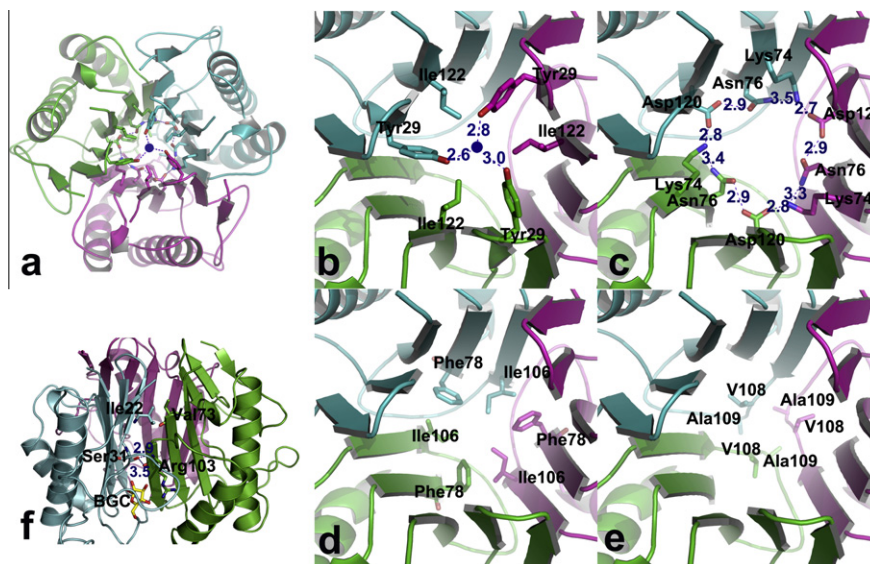
Fig. 2. Panel a is the whole barrel-like cavity of PSPTO-PSP. The view orientation of the trimer is from top to bottom. Three monomers are colored green, blue and pink, respectively. The water is represented by blue sphere; the carbon sticks are colored as its own monomer. Oxygen is red and nitrogen is blue. The hydrogen bonds are shown as purple dash line. Panels b–e show the cover, hydrophilic layer, hydrophobic layer and the bottom of the barrel-like cavity, respectively. The distance of the hydrogen bonds in the cover and hydrophilic layer is marked. Panel f shows the interface between adjoining subunits. The carbon of the glucose is colored yellow and the oxygen is colored red. The hydrogen bonds and its distances between Arg103 and Ser31 are shown as blue dash line and marked. (For interpretation of the references to color in this figure legend, the reader is referred to the web version of this article.)

the walls of the barrel, and further separated the deep cavities from the barrel-like cavity (Fig. 2f).

3.3. Comparison of homologous structures

Alignment of eight homologous sequences of members of the YjgF/YER057c/UK114 family from different species, ranging from single-celled to mutli-cellular organisms, revealed that about 50–90% of the amino acids have similar characteristics and that 15% of the amino acids are 100% conserved (Supplementary Fig. 1). Most of the conserved amino acids interact with glucose in the deep cavities or stabilize the quaternary structure.

These homologous structures were fitted to that of PSPTO-PSP with RMS deviations of 0.66–1.05 Å for the C^{α} positions of the full-length protein (Table 2). This shows that the quaternary structures of YjgF/YER057c/UK114 proteins from different species are highly conserved just as was the case for their sequences. However, the overall structure of PSPTO-PSP is more similar to that of mammalian PSPs than to that of single-celled organisms. This suggested that PSPTO-PSP have the same function with that of mammalian PSPs such as endoribonuclease activity. The structural alignment

of the homologues revealed that PSPTO-PSP appears no conformational changes despite of the bound glucose.

3.4. Active cavity interactions with glucose

The PSPTO-PSP crystal co-crystallized with D-glucose. During structure refining, a large and clear electron density appeared between adjoining subunits in the OMIT map. After test and refinement this was identified as D-glucose. The average B-value of D-glucose in the final structure is 29.6 Å^2.

The amino acids Ser[31], Gly[32], Asn[33], Ile[34], Arg[113], and Arg[103] of neighboring subunits in the active cavity surround the glucose (Fig. 3). Tyr[18] covers the glucose ring, while the bottom of the cavity consists of Pro[112] and Glu[118] from one subunit and Phe[85] from

Table 2
Comparison of YjgF/YER057c/UK114 homologues.

| Protein	Source	Identity	PDB code	R_{msd}
PSPTO-PSP	*Pseudomonas syringae*	100%	3K0T	0.00
YjiF	*E. coli*	0.43	1QU9	1.01
TdcF	*E. coli*	0.42	2UYN	0.99
YabJ	*B. subtilis*	0.49	1QD9	0.89
Hmf1	*S. cerevisiae*	0.44	1JD1	1.03
L-PSP	Rat	0.45	1QAH	1.05
UK114	Goat	0.43	1NQ3	0.70
Hp14.5 (benzoate)	Human	0.45	1ONI	0.66
TdcF (ethylene glycol)	*E. coli*	0.42	2UYJ	0.90
TdcF (propionate)	*E. coli*	0.42	2UYP	1.00
TdcF (Serine)	*E. coli*	0.42	2UYK	0.94
TdcF (2-ketobutyrate)	*E. coli*	0.42	2UYN	0.99
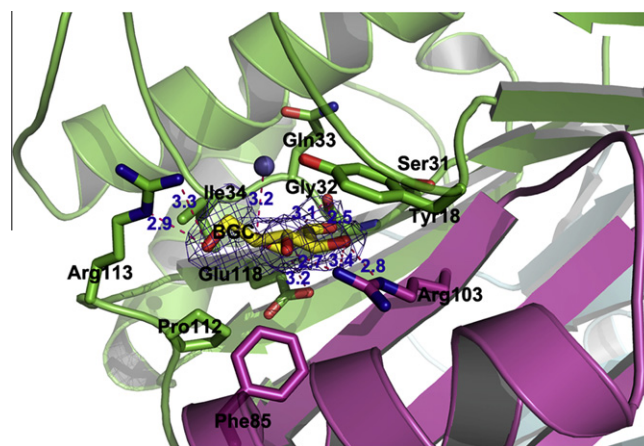
Fig. 3. The active cavity for binding glucose. The color of water and molecules and glucose are as in the Fig. 2. The hydrogen bonds are represented by hot-pink dash lines in order to differentiate from the blue omit map, and its distances are marked; the OMIT map of the glucose is represented by the blue grid line. (For interpretation of the references to color in this figure legend, the reader is referred to the web version of this article.)

its neighboring subunit. The six oxygen atoms from glucose form strong hydrogen bonds with the oxygen atom of the Gly^{32}, the N^E atom of Arg^{113}, the O^{E2} atom of Glu^{118}, atoms N^{H2} and N^E of the Arg^{103} from the neighboring subunit, and a water molecule above the glucose ring (Fig. 3, Table 3). The glucose is stabilized by the strong hydrophobic interactions among the benzene rings, long aliphatic chains, and the glucose ring.

3.5. Comparison of the active cavities of the homologues

All known quaternary structures of YjgF/YER057c/UK114 family members have three cavities for binding ligands or substrates. The human homologue hp14.5 (PDB code 1ONI) can bind benzoate in this cavity, and the E. coli homologue Tdcf can bind serine (PDB code 2UYK), ethylene glycol (PDB code 2UYJ), propionate (PDB code 2UYP), and 2-ketobutyrate (PDB code 2UYN). Comparison of the hydrogen bonds connecting different ligands with the active cavities in the YjgF/YER057c/UK114 family showed that the conserved Arg^{103} of the PSPTO-PSP is a crucial amino acid for different ligands. Arg^{103} makes hydrogen bonds with the ligand via its NE and NH, or O atom, or N atom. As reported, a single mutation of Arg^{107} to Ala^{107} (which aligns to the Arg^{103} of PSPTO-PSP) in hp14.5 results in the dissociation of some trimers into monomers, and greatly decreases ligand binding capacity. Double mutations of Arg^{107} and Pro^{105} in hp14.5 destroy the quaternary structure completely [19]. From previous reports and the structure of this complex, we can confirm that the highly conserved Arg^{103} is a very important amino acid in the active cavity for binding both the ligand and the substrate. It has been reported that mRNA is the substrate of rat L-PSP [9]. The basic amino acid Arg^{103} appears suitable for binding ribonucleotides as substrate.

We compared the active cavities of homologues, including ligand-bound and free-state examples. Even though the angles of the ring planes of Phe^{85} and Tyr^{18} showed some variation, and the position of the Arg^{103} side-chains vary slightly, these conformational changes are most likely not related to ligand binding since free-state homologues also exhibited similar conformational variation. In other words, the conformation of the active site is insensitive to the binding of ligands.

3.6. Implications of glucose binding to PSPTO-PSP

Six compounds bound to HI0719, a member of the YjgF/YER057c/UK114 family, are identified by a targeted screening approach. The compounds are either α-keto acids or α, β-unsaturated acids [19]. The complex structures of some family members bind benzoate, ethylene glycol, serine, propionate, and 2-ketobutyrate [20,21]. Even though so many ligands, only 2-ketobutyrate is reported as an intermediate of the L-serine which is available for isoleucine biosynthesis. Taken together, this report first showed that glucose was a ligand of the YjgF/YER057c/UK114 member.

According to the previous report, when the cell is under low glucose, the translation inhibition activity of the increased PSP can avoid wasting amino acids. This phenomenon is similar and consistent with the characteristics of the stress protein family, such as heat shock proteins HSPs, glucose-regulated proteins GRPs which are responded to the stressors in ER and help repair the proteins hurt by stressors. In addition, PSP is present in ER [22].The change in localization of PSP from the ER to the nucleus suggests that PSP is involved in the cellular response to ER stressors [23]. When the nutrients such as glucose is deficient, they will be recognized as a stress signal which will be transferred by some proteins. In line with previous reports and our structure, PSPs seem have the characteristics similar to the stress proteins.

Moreover, the PSP expression decreased when glucose is supplied to the fasting organism [10]. Glucose supplement retrieve the cells from the stress. The PSPTO-PSP structure in complex with glucose showed that the signals of the stress relief might be transferred by glucose occupying the active cavity of the PSP, which removes the inhibition of PSP on protein synthesis. So we speculated that PSPs might be involved in the cellular response to stressors on one hand, and on the other hand might be responsible to transfer the signals of stress relief to cells.

Appendix A. Supplementary data

Supplementary data associated with this article can be found, in the online version, at doi:10.1016/j.bbrc.2010.05.071.

References

[1] M.R. Christopherson, G.E. Schmitz, D.M. Downs, YjgF is required for isoleucine biosynthesis when Salmonella enterica is grown on pyruvate medium, J. Bacteriol. 190 (2008) 3057–3062.
[2] G. Schmitz, D.M. Downs, Reduced transaminase B (IlvE) activity caused by the lack of yjgF is dependent on the status of threonine deaminase (IlvA) in Salmonella enterica serovar Typhimurium, J. Bacteriol. 186 (2004) 803–810.
[3] J.M. Kim, H. Yoshikawa, K. Shirahige, A member of the YER057c/yjgf/Uk114 family links isoleucine biosynthesis and intact mitochondria maintenance in Saccharomyces cerevisiae, Genes Cells 6 (2001) 507–517.
[4] E. Oxelmark, A. Marchini, I. Malanchi, F. Magherini, L. Jaquet, M.A. Hajibagheri, K.J. Blight, J.C. Jauniaux, M. Tommasino, Mmf1p, a novel yeast mitochondrial protein conserved throughout evolution and involved in maintenance of the mitochondrial genome, Mol. Cell Biol. 20 (2000) 7784–7797.
[5] T. Oka, H. Tsuji, C. Noda, K. Sakai, Y.M. Hong, I. Suzuki, S. Munoz, Y. Natori, Isolation and characterization of a novel perchloric acid-soluble protein inhibiting cell-free protein synthesis, J. Biol. Chem. 270 (1995) 30060–30067.
[6] G. Schmiedeknecht, C. Kerkhoff, E. Orso, J. Stohr, C. Aslanidis, G.M. Nagy, R. Knuechel, G. Schmitz, Isolation and characterization of a 14.5-kDa trichloroacetic-acid-soluble translational inhibitor protein from human monocytes that is upregulated upon cellular differentiation, Eur. J. Biochem. 242 (1996) 339–351.
[7] H. Kanouchi, A. Matsuo, T. Oka, H. Tachibana, K. Yamada, Recombinant perchloric acid-soluble protein suppresses the immunoglobulin production of human–human hybridoma HB4C5 cells, In Vitro Cell. Dev. Biol. Anim. 39 (2003) 263–265.
[8] K. Kaneki, H. Kanouchi, M. Matsumoto, Y. Kawasaki, M. Akuzawa, T. Oka, Down regulation of a novel protein, PSP, in rat hepatoma cdRLh 84-beared tumor, J. Vet. Med. Sci. 65 (2003) 781–785.
[9] R. Morishita, A. Kawagoshi, T. Sawasaki, K. Madin, T. Ogasawara, T. Oka, Y. Endo, Ribonuclease activity of rat liver perchloric acid-soluble protein, a potent inhibitor of protein synthesis, J. Biol. Chem. 274 (1999) 20688–20692.
[10] F. Levy-Favatier, A. Leroux, B. Antoine, B. Nedelec, M. Delpech, Upregulation of rat P23 (a member of the YjgF protein family) by fasting, glucose diet and fatty acid feeding, Cell. Mol. Life Sci. 61 (2004) 2886–2892.

Table 3
Hydrogen bonds in the glucose-bound active cavity of the PSPTO-PSP.

Hydrogen bonds between BGC atoms and protein (Å)		Hydrophobic interaction between BGC and protein (Å)	
BGC-O6–113R-NE	2.9	BGC–18Y	(3.4–3.95)
BGC-O6–113R-NH	2.9	BGC–32G	(3.4–3.9)
BGC-O5–HOH	3.16	BGC–34I	(3.5–3.8)
BGC-O1–32G-O	3.09	BGC–85F	(3.4–3.6)
BGC-O1–118E-OE2	3.15	BGC–112P	(3.7)
BGC-O3–103R-NE of neighbor subunit	2.79	BGC–103R	(3.3–3.9)
BGC-O2–32G-O	2.53	BGC–113R	(3.4–3.9)
BGC-O4–103R-NH2 of neighbor subunit	2.74	BGC–118E	(3.5)

[11] H. Kanouchi, M. Miyamoto, T. Oka, M. Matsumoto, T. Okamoto, S. Tone, Y. Minatogawa, Perchloric acid-soluble protein is expressed in enterocytes and goblet cells in the intestine and upregulated by dietary lipid, Biochim. Biophys. Acta 1760 (2006) 1380–1385.

[12] T. Sasagawa, T. Oka, A. Tokumura, Y. Nishimoto, S. Munoz, M. Kuwahata, M. Okita, H. Tsuji, Y. Natori, Analysis of the fatty acid components in a perchloric acid-soluble protein, Biochim. Biophys. Acta 1437 (1999) 317–324.

[13] Z.O.a.W. Minor, Processing of X-ray diffraction data collected in oscillation mode, Methods Enzymol. 276 (1997) 10.

[14] A.J. McCoy, Solving structures of protein complexes by molecular replacement with Phaser, Acta Crystallogr. D Biol. Crystallogr. 63 (2007) 32–41.

[15] V.S. Lamzin, A. Perrakis, K.S. Wilson, The ARP/wARP suite for automated construction and refinement of protein models, in: M.G. Rossmann, E. Arnold (Eds.), International Tables for Crystallography. Volume F: Crystallography of Biological Macromolecules, Dordrecht, Kluwer Academic Publishers, The Netherlands, 2001, pp. 720–722.

[16] P. Emsley, K. Cowtan, Coot: model-building tools for molecular graphics, Acta Crystallogr. D Biol. Crystallogr. 60 (2004) 2126–2132.

[17] A.A. Vagin, R.A. Steiner, A.A. Lebedev, L. Potterton, S. McNicholas, F. Long, G.N. Murshudov, REFMAC5 dictionary: organization of prior chemical knowledge and guidelines for its use, Acta Crystallogr. D Biol. Crystallogr. 60 (2004) 2184–2195.

[18] M.W.M.R.A. Laskowski, D.S. Moss, J.M. Thornton, PROCHECK: a program to check the stereochemical quality of protein structures export, J. Appl. Cryst. 26 (1993) 9.

[19] E. Mistiniene, N. Pozdniakovaite, V. Popendikyte, V. Naktinis, Structure-based ligand binding sites of protein p14.5, a member of protein family YER057c/YIL051c/YjgF, Int. J. Biol. Macromol. 37 (2005) 61–68.

[20] J.D. Burman, C.E. Stevenson, R.G. Sawers, D.M. Lawson, The crystal structure of *Escherichia coli* TdcF, a member of the highly conserved YjgF/YER057c/UK114 family, BMC Struct. Biol. 7 (2007) 30.

[21] B.A. Manjasetty, H. Delbruck, D.T. Pham, U. Mueller, M. Fieber-Erdmann, C. Scheich, V. Sievert, K. Bussow, F.H. Niesen, W. Weihofen, B. Loll, W. Saenger, U. Heinemann, Crystal structure of Homo sapiens protein hp14.5, Proteins 54 (2004) 797–800.

[22] H. Kanouchi, T. Oka, K. Asagi, H. Tachibana, K. Yamada, Expression and cellular distribution of perchloric acid-soluble protein is dependent on the cell-proliferating states of NRK-52E cells, Cell. Mol. Life Sci. 57 (2000) 1103–1108.

[23] H. Kanouchi, M. Matsumoto, M. Taga, K. Yamada, T. Oka, S. Tone, Y. Minatogawa, Nuclear transfer of perchloric acid-soluble protein by endoplasmic reticulum stressors, Protein Sci. 14 (2005) 2344–2349.